Electronic Supplementary Material (ESI) for Journal of Materials Chemistry A.

Multiporous nanofibers of $SnO_2$by electrospinning for high efficiency dye-sensitized solar cells

QamarWali, AzharFakharuddin, Irfan Ahmed, Mohd Hasbi Ab. Rahim, Jamil Ismail, Rajan Jose*

Nanostructured Renewable Energy Materials Laboratory, Faculty of Industrial Sciences & Technology, Universiti Malaysia Pahang, 26300, Malaysia
*Corresponding author: rjose@ump.edu.my

S1: FESEM of the as-spun nanofiberers

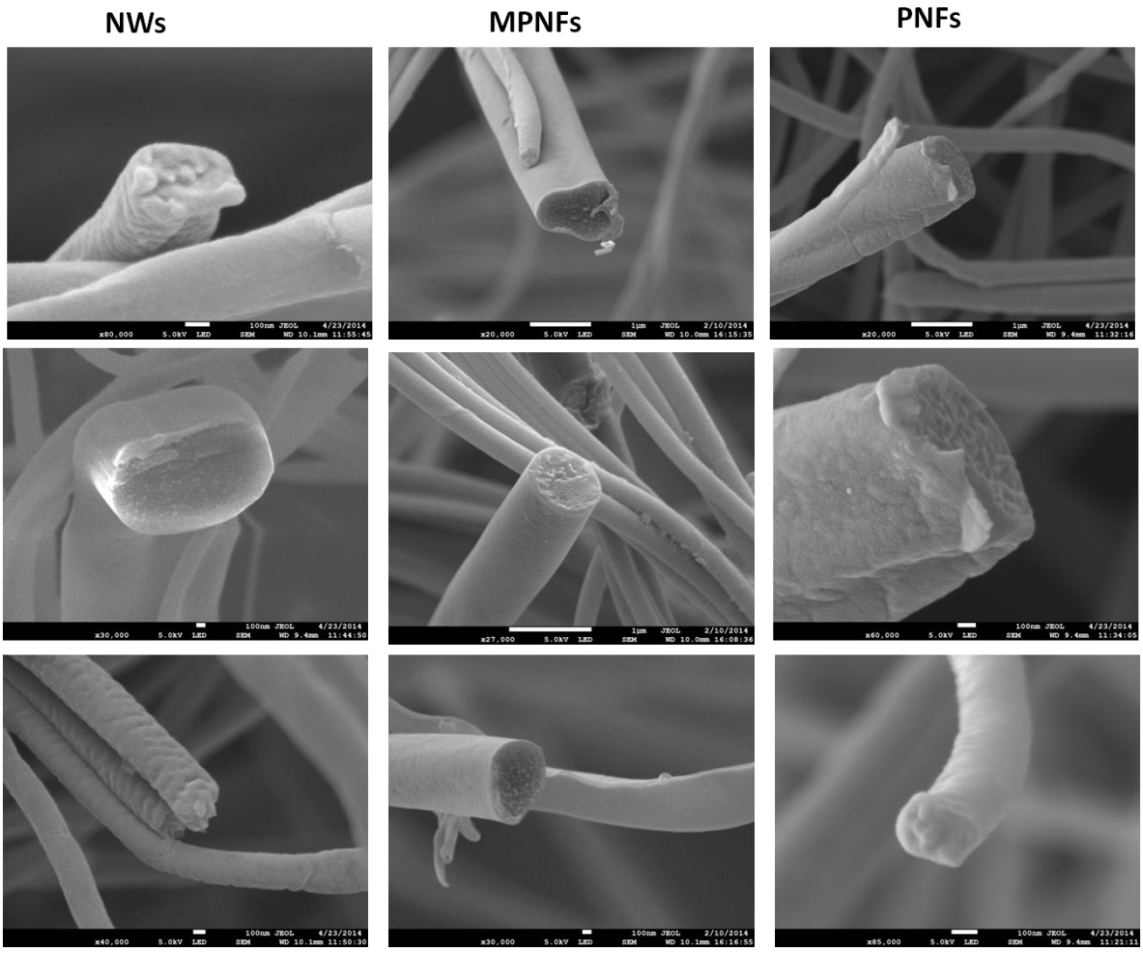

Figure S1: FESEM images of the as spun NWs (a—c), MPNFs (d—f) and PNFs(g—i) respectively.

S2: X-ray diffraction patterns of the as-spun nanofiberers

In an effort to understand the origin of variable porosity of the annealed nanofibers, XRD measurements were carried out. Figure S2 shows the XRD pattern of three typical concentrations C_o, C_1, and C_2 compared with that of pure PVP nanofibers, the tin precursor used during the synthesis, $SnCl_4.5H_2O$, and $Sn(OH)_4$ synthesized by preciptating a clear $SnCl_4.5H_2O$ aqueous solution using ammonium hydroxide. One would observe that crystalline phases are present in the as-spun nanofibers containing the tin precursor, the crystallographic identity of which could not be identified. However, the peaks show a reversal of intensity for C_2 (PNFs) compared to C_1 (MPNFs) indicating the change in orientation of the crystallites – which is expected to be the source of variable porosity upon changing the precursor concentration. Nevertheless, a deep investigation of the mechanism on the formation of variable pores will be investigated and presented elsewhere.

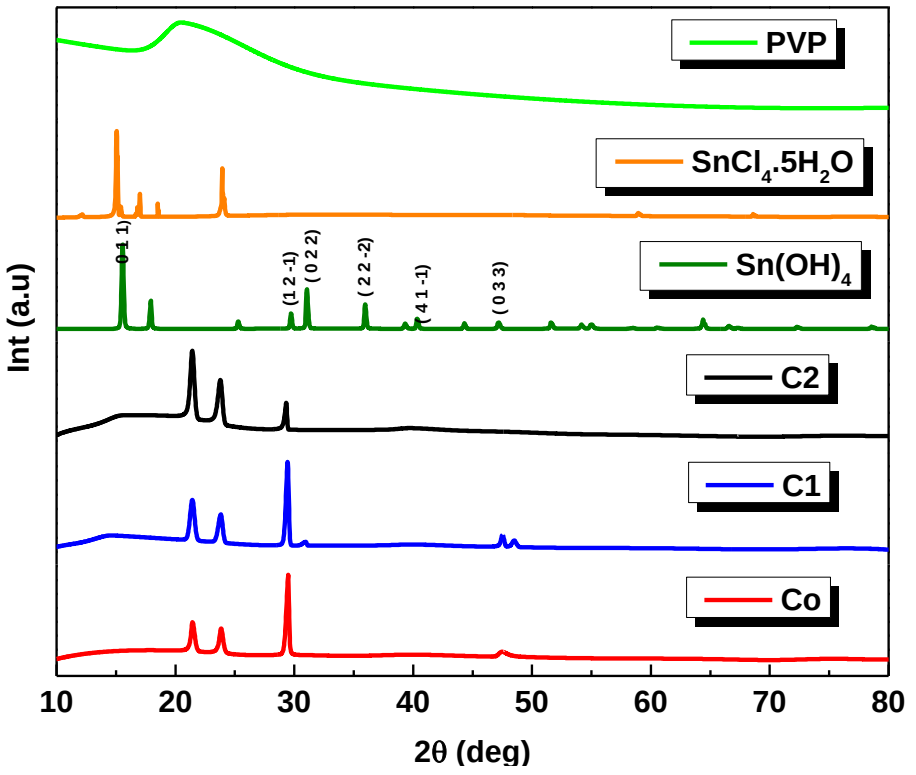

Figure S2: XRD pattern of the as-spun fibers of concentration C_o, C_1, and C_2 compared with that of pure PVP nanofibers, the tin precursor used during the synthesis, $SnCl_4.5H_2O$, and $Sn(OH)_4$ synthesized by preciptating a clear $SnCl_4.5H_2O$ aqueous solution using ammonium hydroxide

S3: Dye loading of the MPNFs, PNFs and P25 DSCs

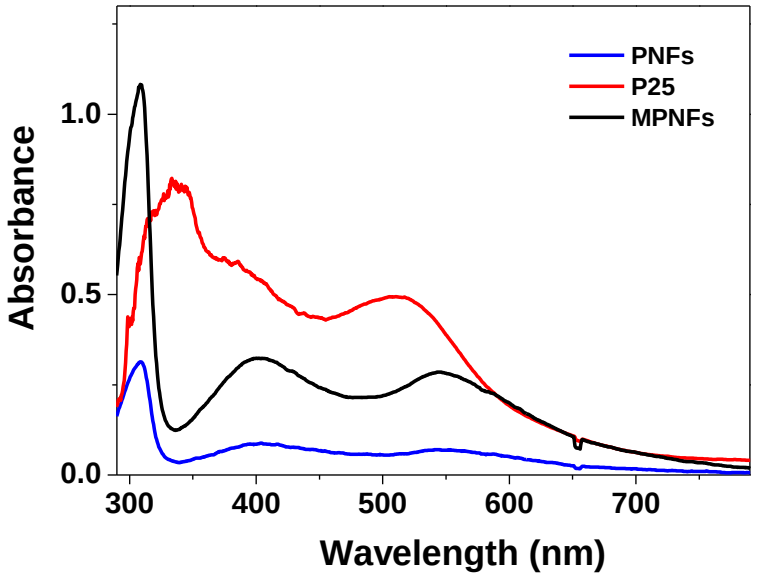

Figure S3: the UV-VIS spectrum of the desorbed dye photoanodes based on PNFs, MPNFs and P25 respectively

The higher current density is a result of two key parameters i.e., high surface area and 1D nature of the nanomaterial. The dye loading of P25 DSCs is the highest, yet the photocurrent is lower than that of MPNFs as the electronic transport in P25 based devices is compromised due to their spherical nature.

S4: Open circuit voltage decay (OCVD)

In order to invistigate the better performance of T-MPNFs DSCs we performed open circuit voltage decay. Under illumination when the V_{OC} stable then switched off the light followed the drop of V_{OC} with time . It is clear from the graph it is clear that T-MPNFs DSCs show slow V_{OC} decay as compare to other NTs and P25 DSCs respectively.

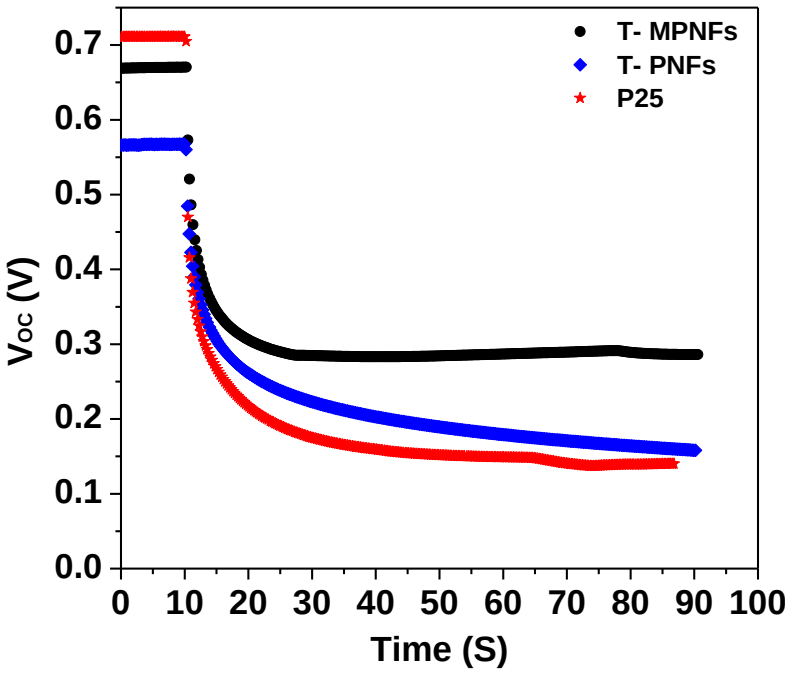

Figure S4: Open circuit voltage decay (OCVD) of the three fabricated DSCs using synthesized SnO_2 T-MPNFs, T-PNFs and commercially available TiO_2 P25 nanoparticles

Extraction of charge transport parameters

The charge transport parameters such as recombination resistance R_{CT}, transport resistance R_T, and chemical capacitance C_μ calculated by fitting the EIS data in Z-view software using bisquert model. The iterations were performed to receive an optimum fit (chi-square $\leq 10^{-5}$) to extract reliable values. These three transport parameters are related to individual components in the transmission line model as shown in following relations, ($R_T = r_t.L$, $R_{CT} = .r_{ct}/L$, and $C_\mu = c_\mu.L$)where L is the cross section thickness of the photoelectrode.

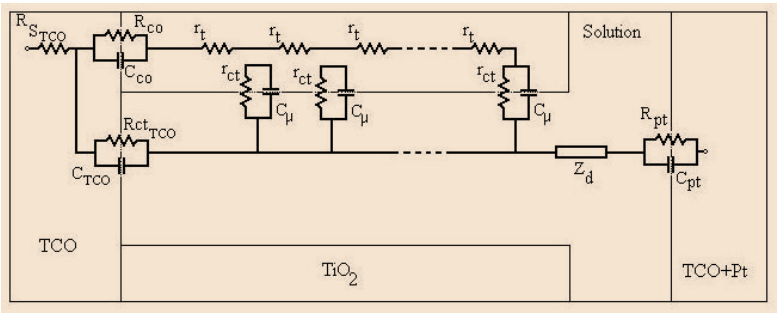

Figure S5: Z-view transmission line model for impedance data analysis

Nyquist and Bode plots of MPNFs and PNFs (without post treatment)

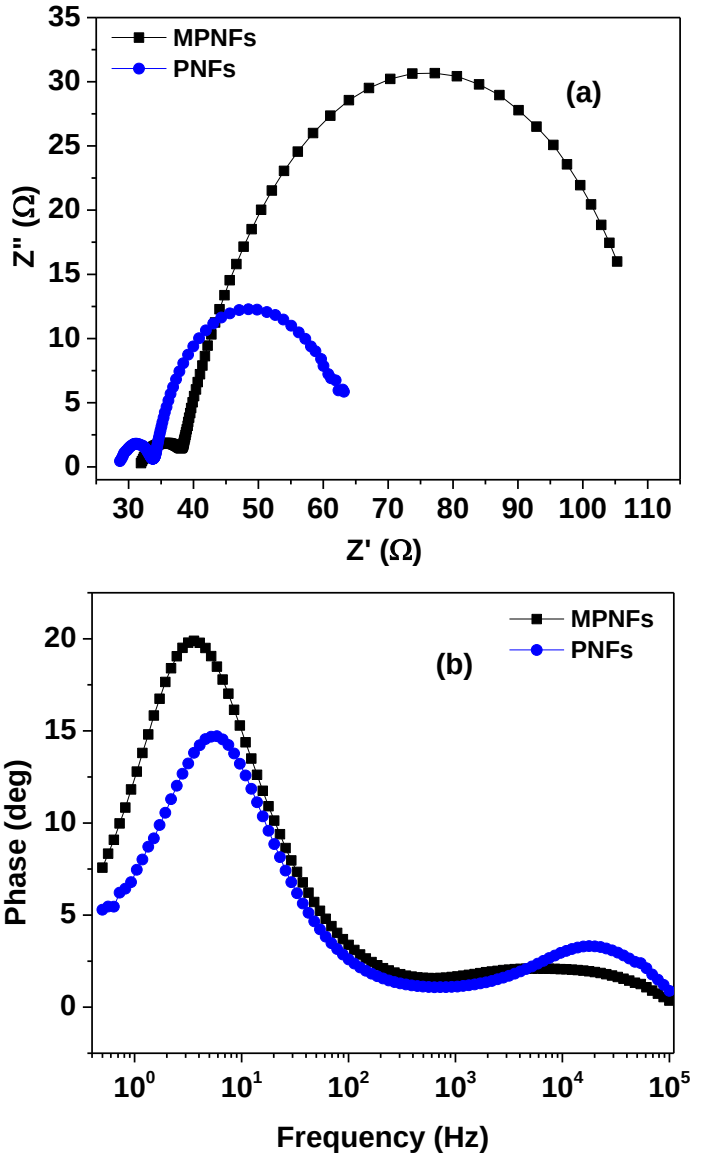

Figure S6: (a) shows the Nyquist plot and (b) demonstrate the bode phase diagram for MPNFs and PNFs respectively

Nyquist and Bode plots of P25 and post treated T-MPNFs and T-PNFs

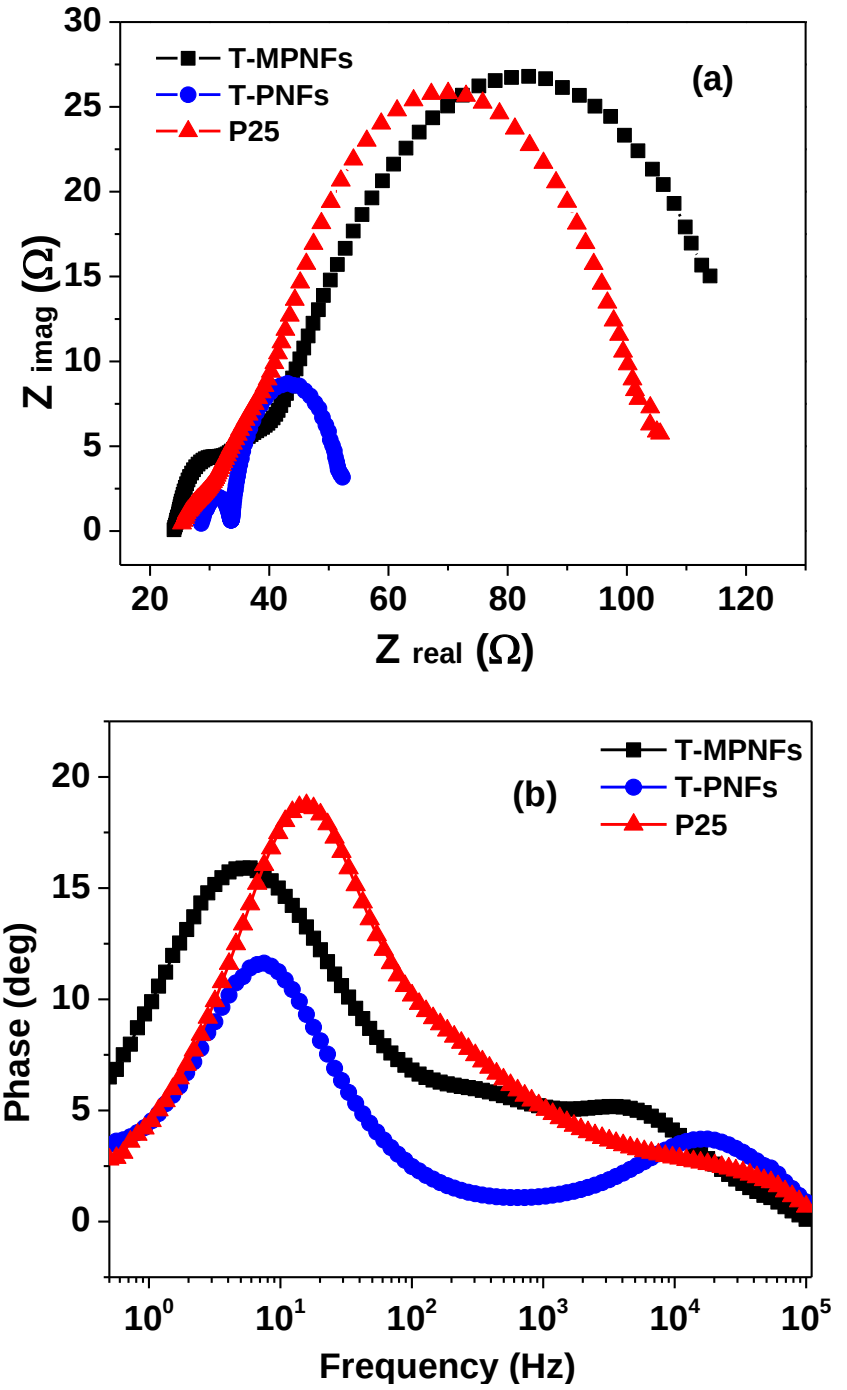

Figure S7: Nyquist (a)and Bode phase (b) diagram for DSCs fabricated using the synthesized T-MPNFs, T-PNFs and commercially availblae TiO_2 P25 nanoparticles respectively.

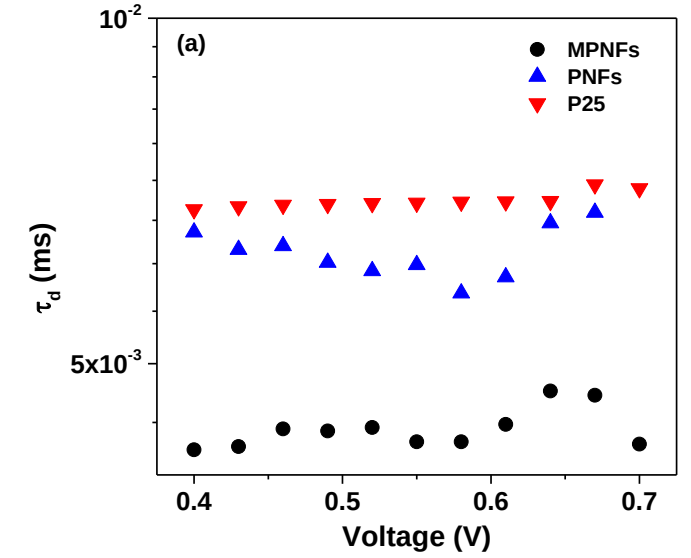
(a)
MPNFs
PNFs
P25
10^{-2}
$5x10^{-3}$
τ_d (ms)
0.4
0.5
0.6
0.7
Voltage (V)

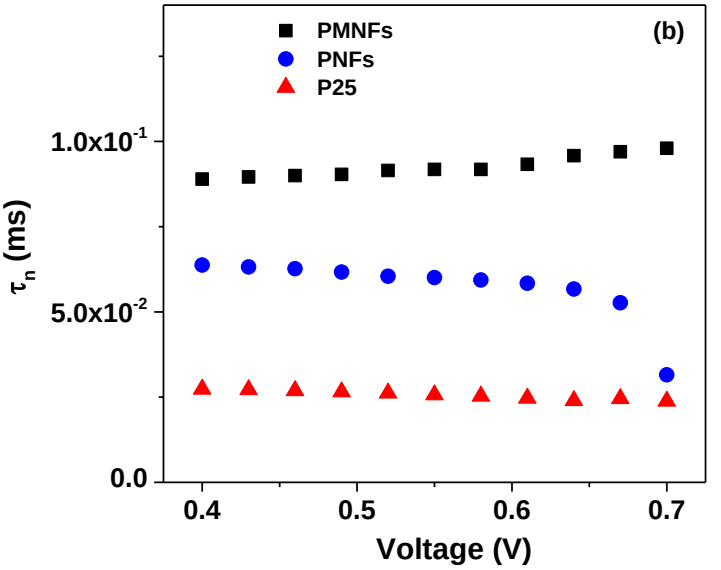
(b)
PMNFs
PNFs
P25
$1.0x10^{-1}$
$5.0x10^{-2}$
0.0
τ_n (ms)
0.4
0.5
0.6
0.7
Voltage (V)

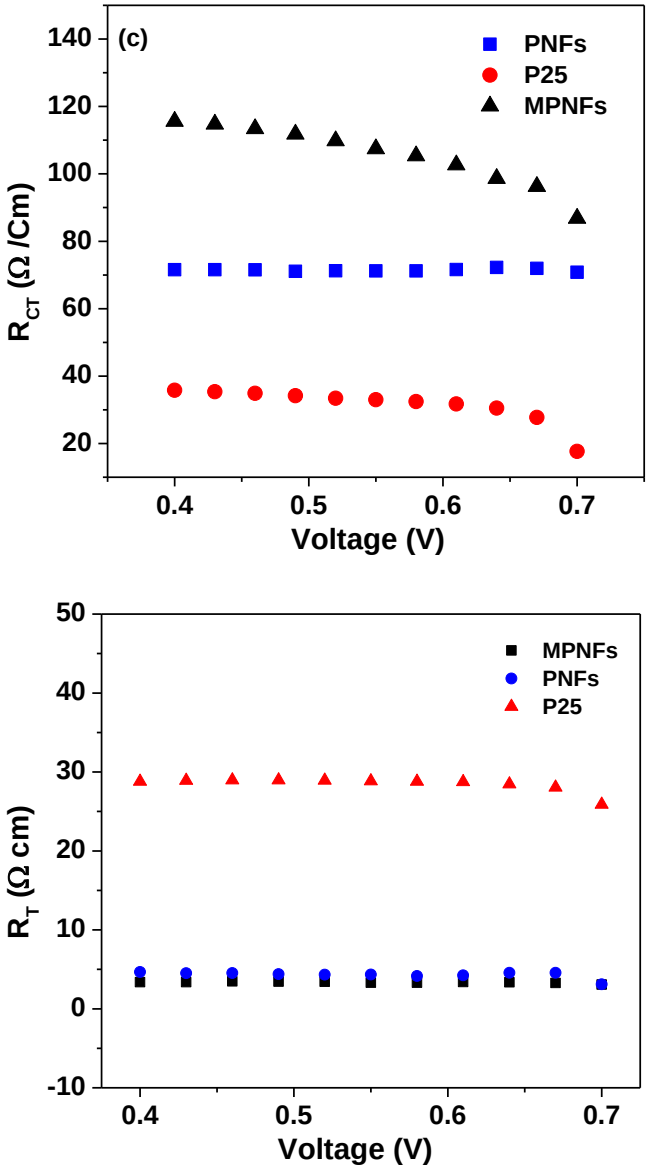

Figure S8: (a) Electron transit time, (b) electron lifetime, (c) recombination resistance, and (d) transport resistance of the three devices.

Extraction of diffusion length

Diffusion length ($L_n = L\sqrt{R_{CT}/R_T}$) is calculated from charge transport and transfer resistance values.sing Z view, the value of individual components (r_t, r_{ct}) is first calculated and then normalized with respect to film thickness using the equations, ($R_T = r_t.L$, $R_{CT} = .r_{ct}/L$) where L is the thickness of the photoelectrode film. The details of each

of these components and their correlation with various photovoltaic parameters is given in our another report.[1]

References

1 Fakharuddin, A.; Ahmed, I.; Khalidin, Z.; Yusoff, M. M.; Jose, R. Charge transport through split photoelectrodes in dye-sensitized solar cells. *J. App. Phys*,.2014, ***115***, 164509.